

# Chapter 17

## Incremental Dynamic Analyses of Steel Moment Resisting Frames with Superelastic Viscous Dampers

Baikuntha Silwal, Osman E. Ozbulut, and Robert J. Michael

**Abstract** This study aims to evaluate the seismic performance of steel moment resisting frames upgraded with shape memory alloy (SMA)-based self-centering viscous dampers. The superelastic viscous damper (SVD) relies on SMA cables for re-centering capability and employs viscoelastic (VE) damper that consists of two layers of a high damped (HD) blended butyl elastomer compound to augment its energy dissipation capacity. First, the design and mechanical behavior of SVDs are described. A nine-story steel frame building is selected for the numerical analyses. The building is analyzed as (1) a conventional special moment resisting frame (SMRF), (2) a dual SMRF-buckling restrained brace (BRB) system, and (3) a SMRF with SVDs. A model of the steel building for each configuration is developed to determine the dynamic response of the structure. The incremental dynamic analysis is used to evaluate the behavior of each building under seven ground-motion records. The analytical results indicate that the SVDs improve the response of steel frame buildings under different level of seismic hazards.

**Keywords** Shape memory alloys • Passive control • Viscoelastic damper • Earthquakes • Steel structures

### 17.1 Introduction

Conventional seismic design approaches rely on the ability of structures to dissipate the input earthquake energy through inelastic deformations in designed regions of the steel frames, implying substantial structural damage and potential extensive residual deformations after a major earthquake [1]. As performance-based earthquake engineering is becoming more prominent, it is important to minimize the damage at multiple seismic hazard levels to achieve the selected performance objectives. McCormick et al. [2] studied the effects of residual drifts on occupants and concluded that residual drifts greater than 0.5 % in buildings may suggest a complete loss of the structure from an economic point of view. In another study, Erochko et al. [3] examined the residual drift response of special moment-resisting frames (SMRFs) and buckling-restrained braced frames (BRBFs). It was found that both types of building systems experience significant residual drifts, with values between 0.8 and 1.5 % for the SMRFs and 0.8–2.0 % for the BRBFs under design-based excitations. By reducing residual drifts of a structure subjected to a seismic event, structural engineers can maximize post-event functionality, reduce the cost to repair the structures, and increase the public safety.

A number of studies have been carried out to develop new structural systems that can provide stable energy dissipation with full re-centering capabilities. Often referred to as self-centering or re-centering, these systems provide a restoring force which is either independent from or acts in addition to energy dissipation capabilities. Christopoulos et al. [4] developed a self-centering energy dissipative bracing system, which combines a friction dissipative mechanism and post-tensioning elements. Experimental tests on the proposed full-scale bracing system were conducted to confirm the repeatable flag-shape hysteretic response. Deierlein et al. [5] proposed a new seismic resisting system that includes controlled rocking, elastic post-tensioning, and replaceable fuses to minimize the damage after an earthquake. Kam et al. [6] studied the effectiveness of advanced flag-shaped systems, where self-centering elements were combined with alternative dissipation elements in series and/or in parallel. It was shown that a seismic-resistant system that consist of a combination of hysteretic and viscous energy

---

B. Silwal • O.E. Ozbulut (✉)

Department of Civil and Environmental Engineering, University of Virginia, Charlottesville, VA, USA

e-mail: [ozbulut@virginia.edu](mailto:ozbulut@virginia.edu)

R.J. Michael

Department of Mechanical Engineering, Gannon University, Erie, PA, USA

dissipation achieve better performance. Eatherton and Hajjar [7] conducted a parametric study to evaluate the necessary maximum re-centering force relative to the yield strength of supplemental energy-absorbing devices as well as the ambient capacity of the structure.

Shape memory alloys (SMAs) have attracted a great deal of attention as a smart material that can be used in seismic protection systems for energy dissipating and re-centering purposes [8]. SMAs behave similarly to linear-elastic materials for small magnitude events, but for moderate and more severe strain levels, SMAs display superelastic behavior from which it can fully recover its original elastic shape. SMAs also exhibit self-centering behavior when permanent deformations in surrounding assemblies afflict the SMA installation; thus, the overall integrity of neighboring structural systems can be maintained. Due to strain hardening of SMA materials, the stiffness of the overall system increases during extreme deformations, which further alleviates deflections in surrounding structural systems. Because of their re-centering capability, SMAs can serve as a valuable component in a seismic control device. Previous studies on SMAs indicate that the quantity of equivalent viscous damping provided by superelastic SMA wires or bars is not sufficient to render the use of SMAs as the sole damping device implemented in a tall structure subjected to severe dynamic loadings [9]. Therefore, several researchers have explored the development of SMA-based control devices with supplemental energy dissipation capabilities [10–12].

This paper investigates the performance of an SMA-based control device, where SMA elements were used in combination with a viscoelastic element in parallel. Compared with conventional structural control devices, the proposed superelastic viscous damper (SVD) is an attractive alternative in both performance and design efficiency. First, a description of the SVDs is provided and the effect of different design parameters on the behavior of the device is studied. Then, a nine-story steel building is designed as conventional special moment resisting frame and with SVDs. For comparison purposes, the steel building is also designed with buckling restrained braces (BRB). Incremental dynamic analyses are conducted using seven ground motion records. The results are analyzed in terms of peak interstory drift, peak floor acceleration, and residual interstory drifts.

## 17.2 Superelastic Viscous Damper

The Superelastic Viscous Damper combines re-centering capabilities of shape memory alloys with the energy dissipation ability of viscoelastic devices. The 3D renderings of the SVD and schematic diagrams of the device in the undeformed and deformed positions are given in Fig. 17.1. The module comprises two high damped butyl elastomer compounds, sandwiched between and bonded to three identical steel plates and installed SMA cables. Each SMA cable forms a continuous loop; wrapping the loops around the outer two plates improves compactness and efficiency. Whether the device itself undergoes a compressive or tensile loading, the configuration ensures that the SMA elements will remain under tension. Along the top and bottom of the device, the wires are threaded through guides, which ensure that the wires remain parallel to the direction of shear deformation in the elastomer layers. As the device moves through its design displacements, the SMA cables apply a re-centering force to the center plate through a second set of wire guides. Composed of three C-channels, two angle brackets, and four crescent-shaped steel sections (one for each strand), each guide distributes the design loads over a longer length of wire (the arc-length of each crescent, compared to the thickness of the center plate) in order to eliminate problematic stress concentrations.

Figure 17.2 shows the typical force-deformation curves of the SVD and its subcomponents. In the SVD, SMA elements are mainly used for its re-centering capability and the viscoelastic device is mainly employed to dissipate seismic energy. By a judicious specification of design parameters of each individual component, a re-centering device with enhanced energy dissipation can be realized.

## 17.3 Building Description

To investigate the seismic performance of the SVD dampers, a nine-story building is selected from the SAC steel project for numerical simulations. The selected steel moment resisting frame is designed as an office building located on a stiff-soil site (Site Class D) in Seattle, Washington. It includes a basement level in addition to the nine stories above the ground level. A floor plan and elevation of the nine-story building are shown in Fig. 17.3. The elevation and floor plan, gravity loads, and seismic mass of the model are identical with the SAC Steel Frame Project [13]. The lateral force resisting system consists of

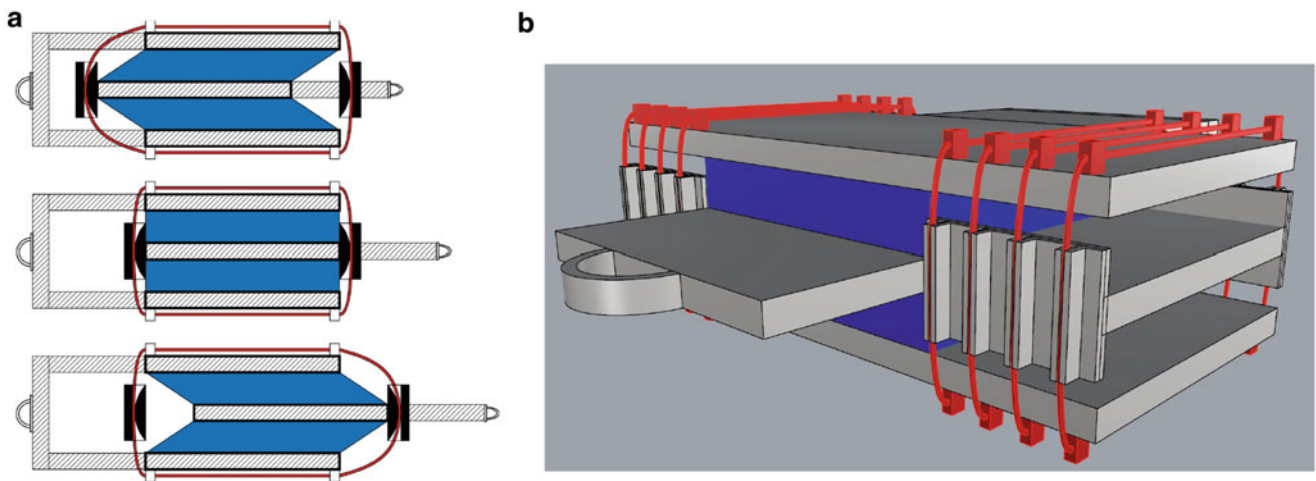


**Fig. 17.1** (a) A schematic diagram of SVD at its undeformed and deformed positions, and (b) 3D Rendering of SVD

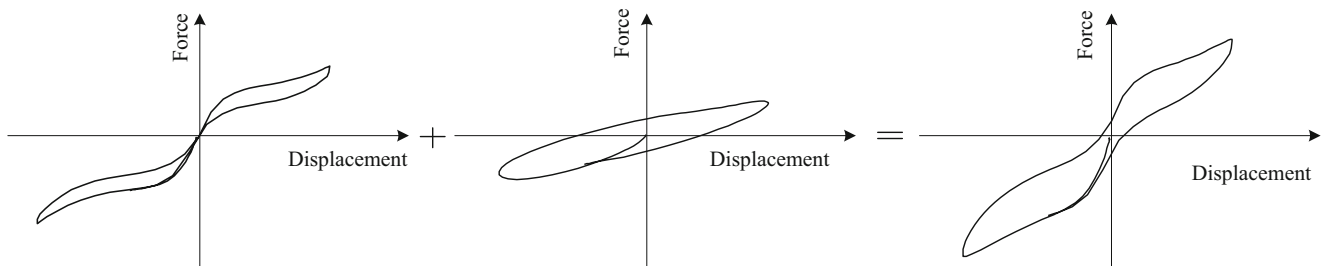


**Fig. 17.2** Force-deformation curves of the SVD and its sub-components

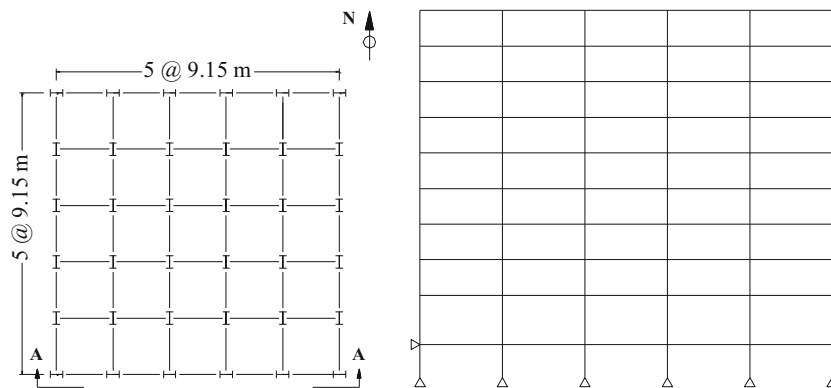


**Fig. 17.3** Plan and elevation of the nine-story steel frame building

two code compliant special steel moment resisting frame in each direction. This study analyzes one of the moment resisting frames in the E-W direction. All columns are assumed to be pinned at the base and the exterior columns are also restrained laterally at the ground level.

The design of the Seattle nine-story moment resisting frame is governed by seismic loads and is compliant with ASCE/SEI 7–10 [14] to satisfy both the strength and drift requirements. The seismic masses used for the analysis of the structures are assigned as  $1.01 \times 10^6$ ,  $9.89 \times 10^5$ , and  $1.07 \times 10^6$  kg for floor level 2, floor levels 3–9, and roof level, respectively. Based on the Seismic Design Category (SDC) D, the following design response spectral values are assigned to the site:  $S_{DS} = 0.912$  g and  $S_{DI} = 0.530$  g for the design basic earthquake (DBE), and  $S_{MS} = 1.368$  g and  $S_{MI} = 0.795$  g for the maximum considered earthquake (MCE). ASCE/SEI 7–10 procedure is employed to develop target spectra for DBE and MCE levels. The response

**Table 17.1** Seven ground motion records used in the design

No.	Earthquake	Station name	Magnitude ( $M_w$ )	Distance (km)	Peak ground acceleration (g)
1	San Fernando (1971)	LA-Hollywood	6.6	22.8	0.19
2	Imperial Valley-06 (1979)	Elcentro array	6.5	12.6	0.37
3	Loma Prieta (1989)	Gilroy array	6.9	12.2	0.37
4	Superstition Hills-02 (1987)	El Centro Imp.	6.5	18.2	0.26
5	Northridge (1994)	Canyon Country	6.7	12.4	0.40
6	Duzce, Turkey (1999)	Duzce	7.1	12.0	0.81
7	Kocaeli, Turkey (1999)	Bolu	7.5	15.4	0.36

**Table 17.2** Members of steel moment resisting frames

Story	SMRF			SMRF with BRB			SMRF with SVDs		
	Exterior columns	Interior columns	Girders	Exterior columns	Interior columns	Girders	Exterior columns	Interior columns	Girders
1	W18 × 311	W18 × 311	W21 × 201	W18 × 311	W18 × 311	W21 × 201	W18 × 311	W18 × 311	W21 × 201
2	W18 × 311	W18 × 311	W21 × 201	W18 × 311	W18 × 311	W21 × 201	W18 × 311	W18 × 311	W21 × 201
3	W18 × 311	W18 × 311	W21 × 201	W18 × 258	W18 × 258	W21 × 166	W18 × 258	W18 × 258	W21 × 166
4	W18 × 311	W18 × 311	W21 × 201	W18 × 258	W18 × 258	W21 × 166	W18 × 258	W18 × 258	W21 × 166
5	W18 × 283	W18 × 283	W21 × 182	W18 × 192	W18 × 211	W21 × 132	W18 × 192	W18 × 211	W21 × 132
6	W18 × 283	W18 × 283	W21 × 182	W18 × 192	W18 × 211	W21 × 132	W18 × 192	W18 × 211	W21 × 132
7	W18 × 234	W18 × 234	W18 × 192	W18 × 130	W18 × 143	W18 × 106	W18 × 130	W18 × 143	W18 × 106
8	W18 × 234	W18 × 234	W18 × 192	W18 × 130	W18 × 143	W18 × 106	W18 × 130	W18 × 143	W18 × 106
9	W18 × 192	W18 × 192	W18 × 175	W18 × 86	W18 × 86	W18 × 65	W18 × 86	W18 × 86	W18 × 65
R	W18 × 192	W18 × 192	W18 × 175	W18 × 86	W18 × 86	W18 × 65	W18 × 86	W18 × 86	W18 × 65

history analysis is adopted to design the structure using a total of seven ground motions that are selected from PEER NGA database [15] as shown in Table 17.1 and scaled according to ASCE/SEI 7–10. The selected column and beam sections are given in Table 17.2. The fundamental period of the nine-story special moment resisting frame is 2.44 s.

In order to comparatively assess the seismic performance of superelastic viscous dampers (SVDs), the nine-story building is also designed with SVDs and traditional BRBs. First, the steel frame is designed to meet all strength and section property requirements by reducing stiffness of beam and columns as given in Table 17.2. This lighter frame design complies with the strength requirements but does not satisfy the prescribed story drift requirements. To comply with the current design requirements, the modified frame is retrofitted with SVDs to satisfy the story drift requirements set by the current design standards, prescribed in Chap. 18 of ASCE/SEI 7–10 for structures with a damping system. Each elastomer compound of the SVD has a dimension of  $406 \times 406 \times 50$  mm. Each SVD employs a total of 8 SMA cables with a diameter of 8 mm and a length of 1210 mm. With these design parameters, the SVD has a displacement capacity of 100 mm and a maximum force capacity of 300 kN. The equivalent viscous damping ratio of a single damper is about 10 %. The SVDs are installed into the second and fourth bays of each story. A nonlinear response-history analysis procedure is adopted to design the frame with SVDs. From the nonlinear response history analyses, the number of dampers at each bay is selected to be 10. Similarly, the lighter frame is also retrofitted with the BRBs to meet story drift requirements as per ASCE/SEI 7–10. The BRB frame is designed using the nonlinear response-history analysis procedure considering the seven ground motion records shown in Table 17.1. The yield stress of the BRB used in the design is 260 MPa. The higher capacity of the BRB is used in the lower five floors above the ground level and the lower capacity is used in remaining top floors. The yield forces of the BRB are 550 kN up to fifth floor from the ground level and 365 kN capacity in the upper four floors. The fundamental periods of the nine-story frame upgraded with SVD and with BRB are 2.26 and 2.04 s, respectively.

## 17.4 Analytical Models

Individual analytical models for the nine-story frame with and without retrofitting devices are developed as two-dimensional frame in the Open System for Earthquake Engineering Simulation (OpenSees) [16]. Based on the concentrated plasticity concept, the beam and column elements are modeled with elastic beam column elements connected by zero-length inelastic plastic hinges employing the modified Ibarra-Krawinkler deterioration model [17]. The modified Ibarra-Krawinkler

deterioration model considers bilinear hysteric response behavior. The cyclic deterioration model parameters of the zero-length rotational springs are assigned based on the model parameters developed by Lignos and Krawinkler [18]. The deterioration characteristics of the rotational springs are indicated by yield strength, post-capping strength, unloading stiffness, and reloading stiffness. The moment-rotation curve is characterized by the elastic stiffness, plastic rotation, a post-capping plastic rotation capacity and the corresponding residual strength. To capture the important panel zone deformation modes, the panel zones are modeled considering the shear distortion in beam-column joints using Krawinkler model [19]. The Krawinkler model includes four rigid links and a rotational spring at the upper right corner to represent shear distortion in the panel zone. The nonlinear plastic hinges are created in beams at an offset from the interface of the panel zone and the beam element while the column plastic hinges are assigned at the face of the panel zone and the column element. To account for P-delta effects, a leaning column is linked to each model with elastic beam-column elements and connected to the model with an axially rigid truss element at each story level. The model assumes Rayleigh damping with a 2 % damping ratio for the first and second modes.

The superelastic viscous damper (SVD) is developed in OpenSees program by combining uniaxial self-centering material property to represent the SMAs and the Maxwell material property to model the elastomeric compound. The superelastic component of the SVD is represented by the finite length element with a uniaxial self-centering material property to capture the hysteric response of the NiTi SMA cable. The self-centering material exhibits flag-shaped hysteric response and also considers the post-transformation hardening behavior with a stiffness equals to the initial stiffness. The experimental test results of SMAs and HD butyl compound reported in Ozbulut et al. [20] are used to develop model parameters for the SMA and elastomeric compound. The model parameters selected for the self-centering material are initial stiffness  $k_1 = 2.915$  kN/mm, post-activation stiffness  $k_2 = 0.994$  kN/mm, forward activation force  $SigAct = 53.047$  kN, post-transformation hardening stiffness = 2.915 kN/mm, and ratio of forward to reverse activation force  $\beta = 1.0$ . Similarly, the Maxwell model parameters are elastic spring coefficient  $K = 1.43$  kN/mm, viscous damping coefficient  $C = 1.00$  kN(s/mm), and nonlinear exponent coefficient  $\alpha = 0.8$ .

The buckling restrained braces are modeled in OpenSees software using inelastic corotTruss element which resists only axial force and deformation. The BRB commonly used in practice varies cross-section from small in the core section and large at the end connections. To reasonably represent the equivalent behavior of the braces, a constant cross-sectional area is employed to the entire length of the truss element. In the constant cross-section model, the modified elastic stiffness and the modified yield strength are assigned to account for the change in BRB area. The elastic stiffness of the BRB is modified according to Ozborrow [21]. The yield strength of the BRB in the truss element is modified to match experimental results by Coy [22]. A bilinear hysteric material model is incorporated using steel02 material to capture the yield behavior of BRB elements. The steel02 material model considers a uniaxial Giuffre-Menegotto-Pinto model with isotropic strain hardening behavior.

## 17.5 Incremental Dynamic Analyses

To evaluate the performance of the steel frames considered in this study up to collapse, incremental dynamic analyses are conducted using seven earthquake records given in Table 17.1. A scale factor of one indicates that the average spectra of seven ground motions are scaled to match the DBE level seismic hazard at the fundamental frequency of the steel moment resisting frame. Peak interstory drift and peak floor absolute acceleration are considered as performance measures. Figures 17.4 and 17.5 show IDA curves for the conventional moment resisting frame and BRB and SVD systems. The figures provide the traces for individual ground motions as well as an average of all ground motions considered here. It can be seen that the SVD system experiences considerably lower interstory drifts compared with other seismic force resisting systems, especially at higher seismic intensity levels. The peak floor acceleration responses of three systems are similar while the SMRF system possesses slightly larger values. The increase in the acceleration response at very high intensity levels for the SVD system can be attributed to the post-transformation hardening behavior of SMA elements.

In addition to IDA curves, the distribution of the peak interstory drift, peak residual story drift and peak floor acceleration over the height of the building are computed for three lateral systems. Figures 17.6 and 17.7 provide the response of each system to individual ground motion records at the DBE level and MCE level, respectively. To facilitate performance assessment of SMRF, BRB and SVD systems comparatively, average response of seven records for each system at the DBE level and MCE level is provided in Figs. 17.8 and 17.9, respectively. It can be seen that the SVD system has the lowest interstory drift and acceleration response values at the MCE level compared to other two lateral systems. The SVD system also has minimal residual drifts at both the DBE and MCE levels, whereas especially BRB system has significant residual deformations.

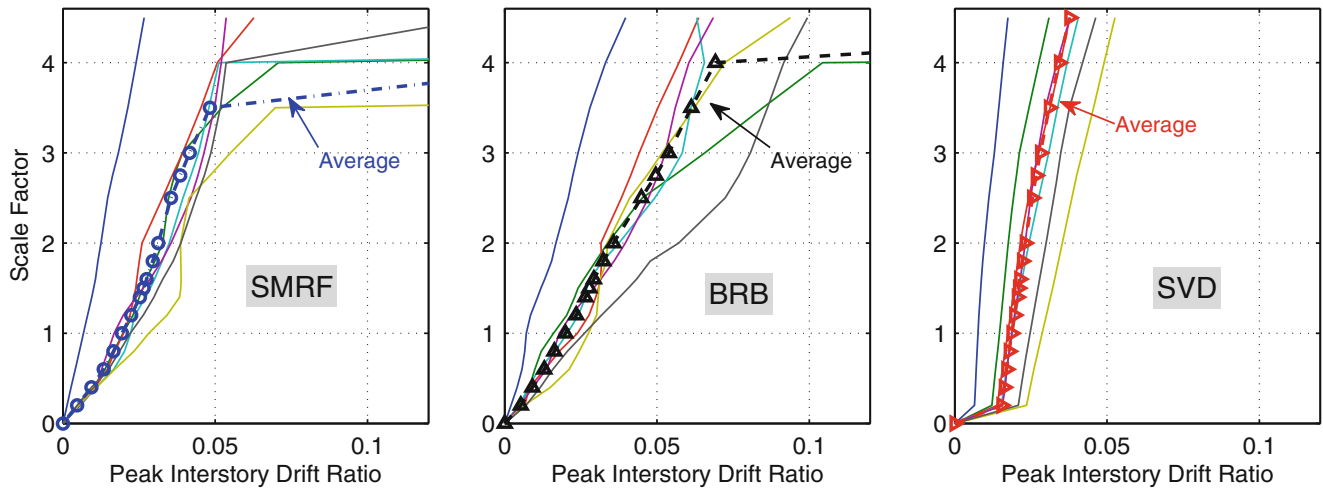


Fig. 17.4 IDA curves for SMRF, BRB and SVD systems at DBE level—peak interstory drift ratio

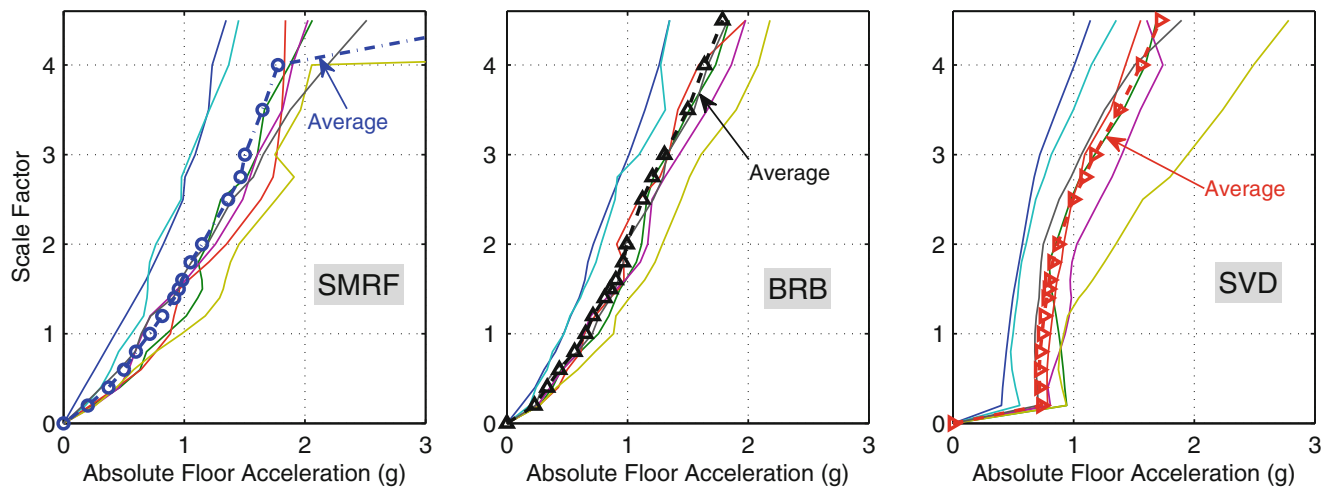
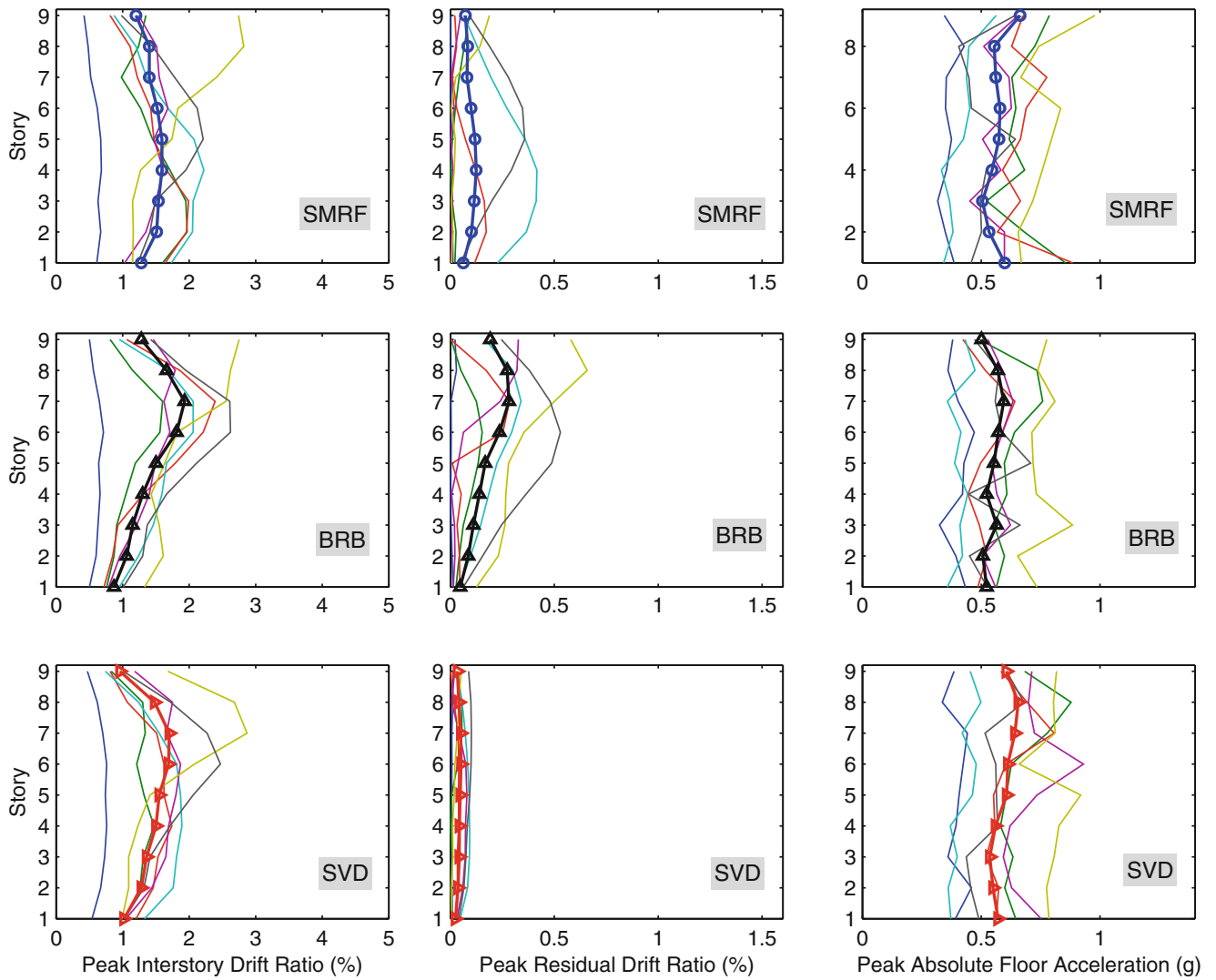


Fig. 17.5 IDA curves for SMRF, BRB and SVD systems at MCE level—peak absolute floor acceleration

## 17.6 Conclusions

In this study, comparative seismic performance assessment of a nine-story steel frame structure designed (1) as special moment resisting system, (2) with buckling restrained braces, and (3) with superelastic viscous devices is conducted. The superelastic viscous dampers leverage the inherent re-centering capability of shape memory alloys and energy dissipation ability of an elastomer compound for superior seismic performance. A heavily damped butyl compound, which provides high damping at low stiffness, is considered for the viscoelastic component of the hybrid damper. Incremental dynamic analysis approach is employed to explore the behavior of nine-story steel building with three different design configurations. Performance of each system in mitigating response of steel frame buildings under DBE and MCE level seismic loads is also assessed. Results show that the superelastic viscous dampers can effectively control the peak drift and acceleration response of steel frames at multiple seismic hazard levels while minimizing residual drifts.



**Fig. 17.6** Profiles of peak response quantities at DBE level for each frame under individual ground motion records

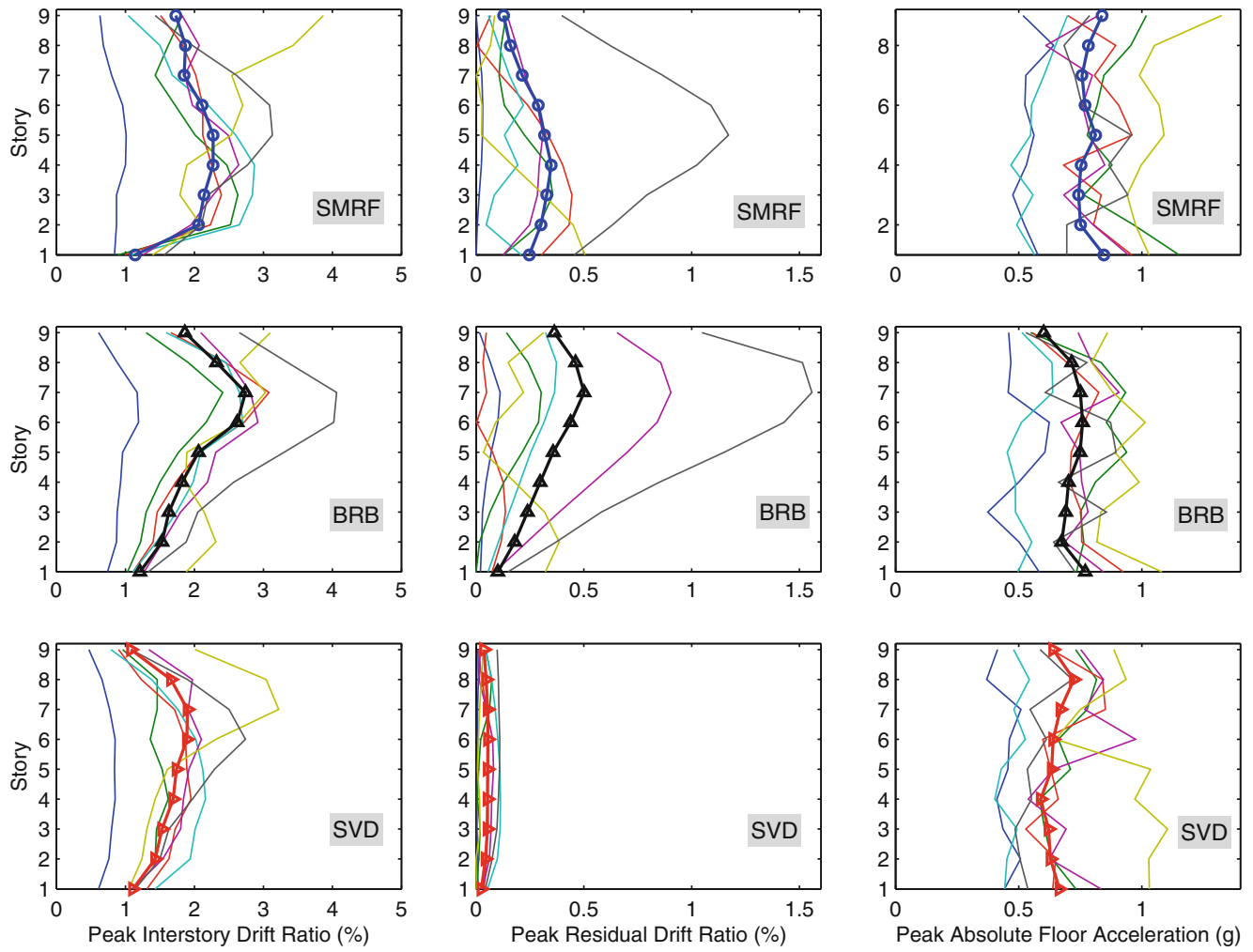


**Fig. 17.7** Profiles of peak response quantities at MCE level for each frame under individual ground motion records

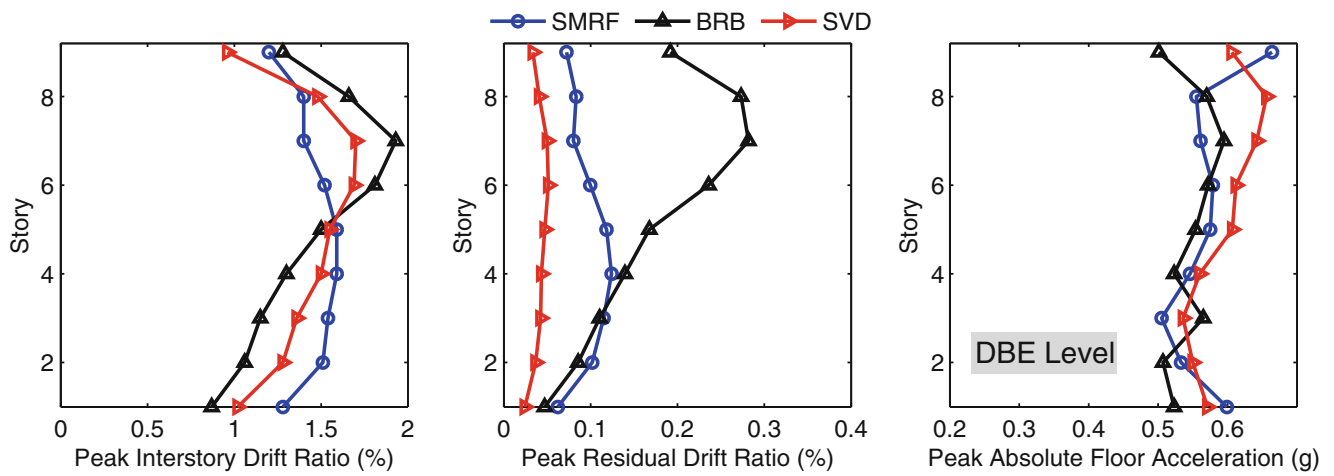


**Fig. 17.8** Envelopes for average of peak response quantities for SMRF, BRB, and SVD systems at DBE level



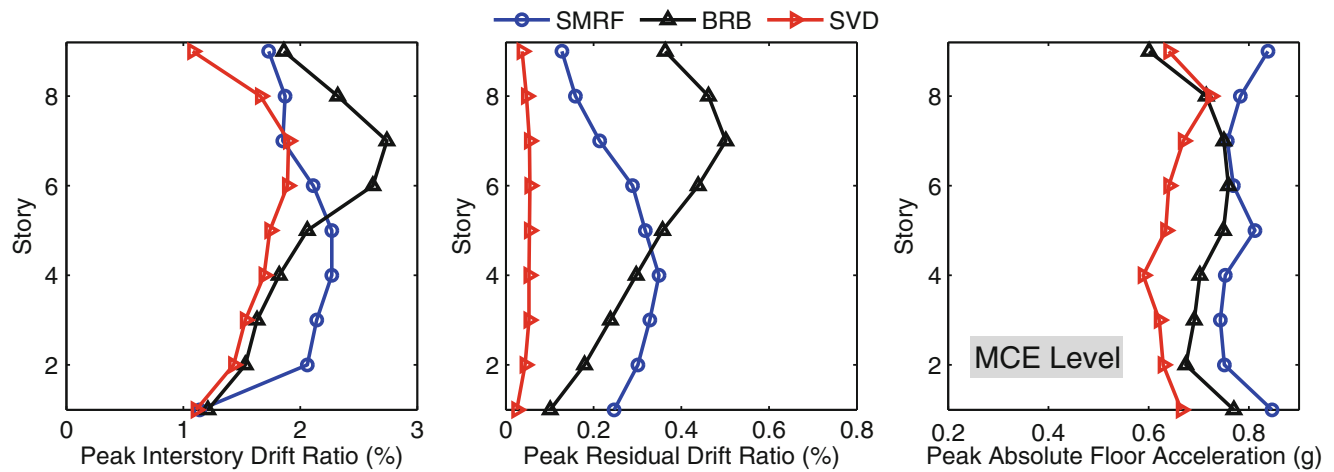


Fig. 17.9 Envelopes for average of peak response quantities for SMRF, BRB, and SVD systems at MCE level

## References

1. Soong, T.T., Dargush, G.F.: *Passive Energy Dissipation System Structural Engineering*. Wiley, Chichester (1997)
2. McCormick, J., Aburano, H., Ikenaga, M., Nakashima, M.: Permissible residual deformation levels for building structures considering both safety and human elements. In: Proc. 14th World Conf. Earthquake Engineering, Seismological Press of China, Beijing, Paper ID 05-06-0071 2008
3. Erochko, J., Christopoulos, C., Tremblay, R., Choi, H.: Residual drift response of SMRFs and BRB frames in steel buildings designed according to ASCE 7–05. *J. Struct. Eng.* **137**(5), 589–599 (2010)
4. Christopoulos, C., Tremblay, R., Kim, H.J., Lacerte, M.: Self-centering energy dissipative bracing system for the seismic resistance of structures: development and validation. *J. Struct. Eng.* **134**(1), 96–107 (2008)
5. Deierlein, G., Krawinkler, H., Ma, X., Eatherton, M., Hajjar, J., Takeuchi, T., Midorikawa, M.: Earthquake resilient steel braced frames with controlled rocking and energy dissipating fuses. *Steel Const.* **4**(3), 171–175 (2011)
6. Kam, W.Y., Pampanin, S., Palermo, A., Carr, A.J.: Self-centering structural systems with combination of hysteretic and viscous energy dissipations. *Earthq. Eng. Struct. Dyn.* **39**(10), 1083–1108 (2010)
7. Eatherton, M.R., Hajjar, J.F.: Residual drifts of self-centering systems including effects of ambient building resistance. *Earthq. Spectra* **27**(3), 719–744 (2011)
8. Ozbulut, O.E., Hurlbauss, S., Desroches, R.: Seismic response control using shape memory alloys: a review. *J. Intell. Mater. Struct.*, **22**, 1531–1549 (2011)
9. Ozbulut, O.E., Hurlbauss, S.: Re-centering variable friction device for vibration control of structures subjected to near-field earthquakes. *Mech. Syst. Sig. Process.* **25**, 2849–2862 (2011)
10. Yang, C.S.W., DesRoches, R., Leon, R.T.: Design and analysis of braced frames with shape memory alloy and energy-absorbing hybrid devices. *Eng. Struct.* **32**, 498–507 (2010)
11. Zhu, S., Zhang, Y.: Seismic analysis of concentrically braced frame systems with self-centering friction damping braces. *J. Struct. Eng.* **134**, 121–31 (2008)
12. Ozbulut, O.E., Hurlbauss, S.: Application of an SMA-based hybrid control device to 20-story nonlinear benchmark building. *Earthq. Eng. Struct. Dyn.* **41**, 1831–1843 (2012)
13. FEMA: State of the Art Report on Systems Performance of Steel Moment Frames Subject to Earthquake Ground Shaking (FEMA 355C). Federal Emergency Management Agency, Washington, DC (2000)
14. ASCE: Minimum Design Loads for Buildings and Other Structures, ASCE 7–10. American Society of Civil Engineers, Reston, Virginia (2010)
15. PEER NGA database. The Pacific Earthquake Engineering Research Center, <http://ngawest2.berkeley.edu>, Pacific Earthquake Engineering Research Center (PEER) (2014)
16. OpenSees. The Open System for Earthquake Engineering Simulation. <http://opensees.berkeley.edu> Pacific Earthquake Engineering Research Center (PEER) (2014)
17. Ibarra, L.F., Medina, R.A., Krawinkler, H.: Hysteretic models that incorporate strength and stiffness deterioration. *Int. J. Earthq. Eng. Struct. Dyn.* **34**(12), 1489–1511 (2005)
18. Lignos, D.G., Krawinkler, H.: A database in support of modeling of component deterioration for collapse prediction of steel frame structures. In: Proceedings, ASCE Structures Congress, Long Beach, California, 18–20 May 2007
19. Gupta, A., Krawinkler, H.: Seismic Demands for Performance Evaluation of Steel Moment Resisting Frame Structures, Technical Report 132. The John A. Blume Earthquake Engineering Research Center, Department of Civil Engineering, Stanford University, Stanford, CA (1999)

20. Silwal, B., Michael, R.J., Ozbulut, O.E.: A superelastic viscous damper for enhanced seismic performance of steel moment frames. *Eng. Struct.* **105**, 152–164 (2015)
21. Ozborrow, G.T.: Optimized distribution of strength in buckling-restrained brace frames in tall buildings. Masters Thesis, BYU, Provo, UT (2009)
22. Coy, B.B.: Buckling-restrained brace connection design and testing. M.S. Thesis, Brigham Young Univ., Provo, UT (2007)